

DISCRETE ELECTROMAGNETISM WITH THE FINITE INTEGRATION TECHNIQUE

M. Clemens and T. Weiland

Darmstadt University of Technology
Fachbereich Elektrotechnik und Informationstechnik
Fachgebiet Theorie Elektromagnetischer Felder
Schlossgartenstrasse 8, D-64289 Darmstadt, Germany

Abstract—The Finite Integration Technique (FIT) is a consistent discretization scheme for Maxwell's equations in their integral form. The resulting matrix equations of the discretized fields can be used for efficient numerical simulations on modern computers. In addition, the basic algebraic properties of this discrete electromagnetic field theory allow to analytically and algebraically prove conservation properties with respect to energy and charge of the discrete formulation and gives an explanation of the stability properties of numerical formulations in the time domain.

1 Introduction

2 Algebraic Properties of the Matrix Operators

3 Algebraic Properties of the Discrete Fields

4 Discrete Fields in Time Domain

5 Conclusion

References

1. INTRODUCTION

All macroscopic electromagnetic phenomena occurring in practice can be mathematically described with the complete set of Maxwell's equations. The Finite Integration Technique (FIT) [1] developed by Weiland in 1977 provides a discrete reformulation of Maxwell's equations in their integral form suitable for computers and it allows to simulate real-world electromagnetic field problems with

complex geometries. This finite volume-type discretization scheme for Maxwell's equations relies on the usage of integral balances and thus allows to prove stability and conservation properties of the discrete fields even before starting with numerical calculations. In particular, such algebraic properties of the discrete formulation enable the development of long-term stable numerical time integration schemes or accurate eigenvalue solvers avoiding spurious modes.

Recently, the language of differential forms and concepts of algebraic topology have been used to study Maxwell's equations restricted to lattices, e.g. in [2], [3], [4]. In the resulting discrete formulations the equations are typically separated in those which are metric-free, arising from topology, and in those which are metric-dependent. They closely resemble (or paraphrase) those discrete formulations of the Finite Integration Technique, which are already established for more than 20 years. This new mathematical background also triggers a corresponding reinterpretation of modern conformal Edge-Finite-Element schemes [5] used in computational electromagnetics, which are usually rather derived starting from mathematical variational formulations [3].

The first discretization step of the FI-method consists in the restriction of the electromagnetic field problem, which usually represents an open boundary problem, to a simply connected and bounded space region $\Omega \in \mathbb{R}^3$, which contains the space region of interest. The next step consists in the decomposition of the computational domain Ω into a (locally) finite number of simplicial cells V_i such as tetra- or hexahedra under the premise that all cells have to fit exactly to each other, i.e. the intersection of two different cells is either empty or it must be a two-dimensional polygon, a one-dimensional edge shared by both cells or a point. This decomposition yields the finite simplicial cells complex G , which serves as computational grid.

Starting with this very general cell-based approach to a spatial discretization it is clear, that the FI-theory is not only restricted to three-dimensional Cartesian meshes. It allows to consider all types of coordinate meshes, orthogonal and non-orthogonal meshes [6], [7]. Also consistent subgridding schemes (corresponding to a local mesh refinement including grid line termination techniques) have been developed [8]. The FI-Technique even extends to non-simplicial cells, as long as the resulting cell complex is homeomorphic to a simplicial cell complex. For practical application such general cell complexes, where the cell edges may be curves, only play a role if they occur as coordinate meshes.

Note that each edge of the cells includes an initial *orientation*, i.e.,

a direction, such that the union of all this cell edges can be described as a *directed graph* [9]. Analogously also polygonal facets of the complex will be associated with a direction.

For the sake of simplicity, however, it is assumed that Ω is brick-shaped in the following description of the FI-technique and that the decomposition is given with a with a tensor product grid for Cartesian coordinates such that we get a cell complex

$$G := \{V_{i,j,k} \in \mathbb{R}^3 \mid V_{i,j,k} := [x_i, x_{i+1}] \times [y_j, y_{j+1}] \times [z_k, z_{k+1}], \\ i = 1, \dots, I-1, j = 1, \dots, J-1, k = 1, \dots, K-1\}, \quad (1)$$

where the nodes (x_i, y_j, z_k) are enumerated with the coordinates i, j and k along the x -, y - and z -axis. This results in the total number of $N_p := I \cdot J \cdot K$ mesh points for $(I-1) \cdot (J-1) \cdot (K-1)$ mesh cells.

After the definition of the grid cell complex G , the further introduction of the FI-theory can be restricted to a single cell volume V_n . Starting with Faraday's law in integral form

$$\oint_{\partial A} \vec{E}(\vec{r}, t) \cdot d\vec{s} = - \iint_A \frac{\partial}{\partial t} \vec{B}(\vec{r}, t) \cdot d\vec{A} \quad \forall A \in \mathcal{R}^3, \quad (2)$$

can be rewritten for a facet $A_z(i, j, k)$ of V_n as the ordinary differential equation

$$\widehat{e}_x(i, j, k) + \widehat{e}_y(i+1, j, k) - \widehat{e}_x(i, j+1, k) - \widehat{e}_y(i, j, k) = \\ - \frac{d}{dt} \widehat{b}_z(i, j, k), \quad (3)$$

as shown in Fig. 1, where the scalar value $\widehat{e}_x(i, j, k) = \int_{(x_i, y_j, z_k)}^{(x_{i+1}, y_j, z_k)} \vec{E} \cdot d\vec{s}$ is the electric voltage along one edge of the surface $A_z(i, j, k)$, representing the exact value of the integral over of the electric field along this edge. The scalar value $\widehat{b}_z(i, j, k) = \int_{A_z(i, j, k)} \vec{B} \cdot d\vec{A}$ represents the magnetic flux, i.e., the integral value over the magnetic flux density, through the cell facet $A_z(i, j, k)$. Note that the orientation of the cell edges will have influence on the signs within (3). It has to be emphasized that equation (3) is an exact representation of (2) for the cell surface under consideration.

The integral formulation of Farady's law (2) is valid for each single facet $A(i, j, k)$ of G and the discrete approach in (3) naturally extends to larger facet areas $A = \cup A(i, j, k)$ due to the relation $\sum \oint_A \vec{E} \cdot d\vec{s} = \oint_A \vec{E} \cdot d\vec{s}$. The same result will hold for surface integrals. This motivates the spatial discretization approach by a finite cell complex chosen within the Finite Integration Technique.

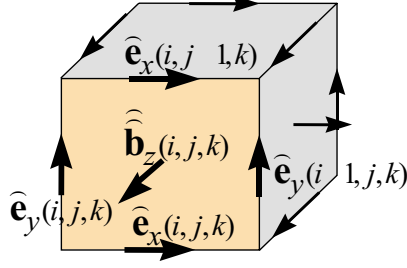


Figure 1. A cell $V_{i,j,k-1}$ of the cell complex G with the allocation of the electric grid voltages \hat{e} on the edges of A and the magnetic facet flux \hat{b} through this surface.

Assuming a lexicographical ordering of the electric voltages $\hat{e}(i,j,k)$ and of the magnetic facet fluxes $\hat{b}(i,j,k)$ over the whole cell complex G and their assembly into column vectors in such a way, that we compose the degrees of freedom first in x -direction, then in y - and z -direction, we get two vectors

$$\hat{\mathbf{e}} := (\hat{e}_{x,n} | \hat{e}_{y,n} | \hat{e}_{z,n})_{n=1,\dots,N_p}^T \in \mathbb{R}^{3N_p} \quad (4)$$

$$\hat{\mathbf{b}} := (\hat{b}_{x,n} | \hat{b}_{y,n} | \hat{b}_{z,n})_{n=1,\dots,N_p}^T \in \mathbb{R}^{3N_p}. \quad (5)$$

The equations (3) of all grid cell surfaces of the complex G can be collected in a matrix form

$$\underbrace{\begin{pmatrix} 1 & \dots & 1 & \dots & -1 & \dots & -1 \\ \dots & \dots & \dots & \dots & \dots & \dots & \dots \end{pmatrix}}_{\mathbf{C} :=} \underbrace{\begin{pmatrix} \hat{e}_{n_1} \\ \vdots \\ \hat{e}_{n_2} \\ \vdots \\ \hat{e}_{n_3} \\ \vdots \\ \hat{e}_{n_4} \end{pmatrix}}_{\hat{\mathbf{e}}} = -\frac{d}{dt} \underbrace{\begin{pmatrix} \vdots \\ \hat{b}_n \\ \vdots \end{pmatrix}}_{\hat{\mathbf{b}}}. \quad (6)$$

The matrix \mathbf{C} contains only topological information on the incidence relation of the cell edges within G and on their orientation, thus it only has matrix coefficients $\mathbf{C}_{i,j} \in \{-1, 0, 1\}$. It represents a discrete *curl*-operator on the grid G .

In terms of algebraic topology the discrete curl operator of FIT is identical to the *coboundary process operator* that is applied to the

cochains of degree one, i.e., the degrees of freedom allocated on one-dimensional cell chains, resulting in a cochain of degree two, i.e., a degree of freedom connected to a two-dimensional cell-surface [2].

The second discrete differential operator to be considered is the *divergence* operator. Its derivation originates from Maxwell's equation describing the non-existence of magnetic charges

$$\iint_{\partial V} \vec{B}(\vec{r}, t) \cdot d\vec{A} = 0 \quad \forall V \in \mathcal{R}^3, \quad (7)$$

which is considered for a cell $V_{i,j,k}$ as shown in Fig. 2.

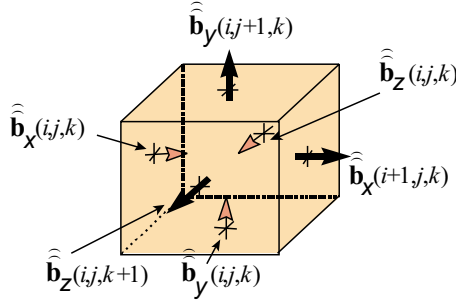


Figure 2. This figure depicts the allocation of the six magnetic facet fluxes which have to be considered in the evaluation of the closed surface integral for the non-existence of magnetic charges within the cell volume.

The evaluation of the surface integral in (7) for the depicted brick cell yields

$$\begin{aligned} -\hat{\mathbf{b}}_x(i, j, k) + \hat{\mathbf{b}}_x(i+1, j, k) - \hat{\mathbf{b}}_y(i, j, k) + \hat{\mathbf{b}}_y(i, j+1, k) \\ - \hat{\mathbf{b}}_z(i, j, k) + \hat{\mathbf{b}}_z(i, j, k+1) = 0, \end{aligned} \quad (8)$$

which is an exact relation for the considered volume.

Again this relation for a single cell can be expanded to the whole

cell complex G and this yields the discrete divergence matrix

$$\underbrace{\begin{pmatrix} & & & \cdots & \cdots & & \\ & -1 & 1 & -1 & 1 & -1 & 1 & . \\ & & & \cdots & \cdots & & & \end{pmatrix}}_{\mathbf{S} :=} \underbrace{\begin{pmatrix} \vdots \\ \widehat{\widehat{b}}_{m_1} \\ \widehat{\widehat{b}}_{m_2} \\ \widehat{\widehat{b}}_{m_3} \\ \widehat{\widehat{b}}_{m_4} \\ \widehat{\widehat{b}}_{m_5} \\ \widehat{\widehat{b}}_{m_6} \\ \vdots \end{pmatrix}}_{\widehat{\mathbf{b}}} = 0. \quad (9)$$

The discrete divergence (*source*) matrix $S \in \mathbb{R}^{N_p \times 3N_p}$ also only depends on the grid topology just as the discrete *curl*-matrix C . It corresponds to the coboundary operator applied to cochains of degree two (surface degrees of freedom) that yields cochains of degree three, a degree of freedom connected to a whole cell volume [2].

The discretization of the remaining two Maxwell equations within the Finite Integration Technique requires the introduction of a second cell complex \tilde{G} which is dual to the primary cell complex G . For the Cartesian tensor product grid G the dual grid \tilde{G} is defined by taking the foci of the cells of G as gridpoints for the mesh cells of \tilde{G} .

For more general, eventually unstructured, cell complexes G it is also possible to take the cell barycenters as boundary vertices for definition of the dual grid cells of \tilde{G} [6], [3].

With this definition it can be ensured that there is a one-to-one relation between the cell edges of G cutting through the cell surfaces of \tilde{G} and vice versa. Along the edges \tilde{L}_k of the so defined dual grid cells we integrate the magnetic field intensities resulting in a magnetomotive force $\widehat{\mathbf{h}}_k = \int_{\tilde{L}_k} \vec{H} \cdot d\vec{s}$ with the physical unit *Ampère*. On the cells surfaces of \tilde{G} the dielectric fluxes and the electric currents are allocated in analogy to electric grid voltages and magnetic facet fluxes on G .

Hence the complete integral of the charge density within a dual cell \tilde{V} can be related to a discrete charge onto the single grid point of the primal grid G placed inside \tilde{V} .

The discretization of Ampère's law in integral form

$$\oint_{\partial \tilde{A}} \vec{H}(\vec{r}, t) \cdot d\vec{s} = \iint_{\tilde{A}} \left(\frac{\partial}{\partial t} \vec{D}(\vec{r}, t) + \vec{J}(\vec{r}, t) \right) \cdot d\vec{A} \quad \forall \tilde{A} \in \mathcal{R}^3 \quad (10)$$

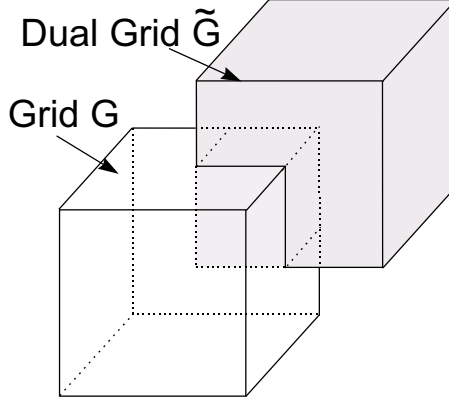


Figure 3. This figure shows the spatial allocation of a cell and a dual cell of the grid doublet $\{G, \tilde{G}\}$.

can be performed for an arbitrary facet \tilde{A} of a dual grid cell \tilde{V} in complete analogy to Faraday's law by summing up the magnetic grid voltages in order to obtain the displacement current and the conductive current through the considered cell facet.

Finally, Gauss' law in integral form can be discretized for the dual grid cells. Both these discretizations for the dual grid cell complex will result in matrix equations featuring the topological grid operators $\tilde{\mathbf{C}}$ for the dual discrete curl and $\tilde{\mathbf{S}}$ for the dual discrete divergence. For the cell complex pair $\{G, \tilde{G}\}$ the complete set of discrete matrix equations, the so-called *Maxwell-Grid-Equations* (MGE) is now given by:

$$\mathbf{C} \widehat{\mathbf{e}} = -\frac{d}{dt} \widehat{\mathbf{b}}, \quad \tilde{\mathbf{C}} \widehat{\mathbf{h}} = \frac{d}{dt} \widehat{\mathbf{d}} + \widehat{\mathbf{j}}, \quad (11)$$

$$\mathbf{S} \widehat{\mathbf{b}} = 0, \quad \tilde{\mathbf{S}} \widehat{\mathbf{d}} = \mathbf{q}. \quad (12)$$

Irrotational electromagnetic fields in Ω can be represented as gradient-fields of scalar potentials according to Poincare's lemma. Within the context of the FI-Technique one deals with electric grid voltages allocated on the cell edges. To represent these as difference of two nodal potential values, discrete potential values $\Phi(i, j, k)$ are allocated onto the intersecting grid mesh points of G , such that the relation

$$-\Phi(i+1, j, k) + \Phi(i, j, k) = \widehat{\mathbf{e}}_x(i, j, k) \quad (13)$$

holds. Collecting these discrete potential values and their relation (13)

into vectors Φ over the whole cell complex G , one obtains the relation

$$\widehat{\mathbf{e}} = -\mathbf{G}\Phi, \quad (14)$$

where the discrete *gradient* matrix $\mathbf{G} = -\widetilde{\mathbf{S}}^T$ indeed is the negative transpose of the dual discrete divergence operator. Analogously, the same procedure can be applied using magnetic potentials on the cell vertices of the dual cell complex \widetilde{G} to derive the discrete gradient matrix $-\mathbf{S}^T$ for the irrotational dual magnetic grid voltages with $\widehat{\mathbf{h}} = -\widetilde{\mathbf{G}}\Psi (= \mathbf{S}^T\Psi)$, where Ψ is a magnetic scalar nodal potential vector.

A discretization has been performed for Maxwell's equations only so far, as the computational domain has been artificially bounded and the information that these equations hold is only about integral state variables which are either allocated on points (potentials), edges (voltages), surfaces (fluxes) or the cell volume (charges). The resulting equations are an exact representation of Maxwell's Equations on a grid doublet.

The approximation of the method itself enters when the integral voltage- and flux state-variables allocated on the two different cell complexes are to be related to each other by the constitutive material equations. In the case of the simple Cartesian tensor product grid the two cell complexes G and \widetilde{G} are dual orthogonal and represent a so-called *Delaunay-Voronoi*-grid doublet. Here the directions associated to the facet and to the dual edge penetrating this facet are identical. In addition with the one-to-one correspondence of the facets and their penetrating dual edges this will result in discrete material matrix relations

$$\widehat{\mathbf{d}} = \mathbf{M}_\varepsilon \widehat{\mathbf{e}} + \widehat{\mathbf{p}}, \quad \widehat{\mathbf{j}} = \mathbf{M}_\kappa \widehat{\mathbf{e}}, \quad \widehat{\mathbf{h}} = \mathbf{M}_\nu \widehat{\mathbf{b}} - \widehat{\mathbf{m}}, \quad (15)$$

featuring only diagonal matrices for diagonal or isotropic material tensors [10]. Here \mathbf{M}_ε is the permittivity matrix, \mathbf{M}_κ is the (usually singular) matrix of conductivities, \mathbf{M}_ν the matrix of reluctivities and $\widehat{\mathbf{p}}$ and $\widehat{\mathbf{m}}$ arise from permanent electric and magnetic polarisations. Within these matrix equations the relations of the degrees of freedom corresponding to the two grid complexes G and \widetilde{G} are described, coupling edge degrees of freedom, so-called *discrete 1-forms*, with dual facet degrees of freedom, so-called *discrete 2-forms*. In differential geometry an isomorphism, which maps a 1-form onto a 2-form (in the manifold \mathcal{R}^3), is called a Hodge operator. Hence the material matrices of the FIT can be dubbed as *discrete Hodge operators* [3] and contain the metrical information of the MGE, i.e., they contain the averaged

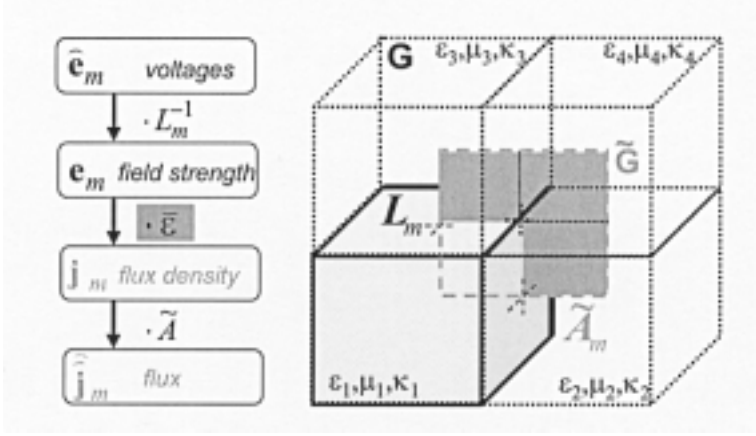


Figure 4. The coupling of the degrees of freedom on G and \tilde{G} is performed in the constitutive material equations. Here, an electric grid voltage $\hat{\mathbf{e}}_m$ allocated on an edge $L_m \in G$ is coupled to a facet flux $\hat{\mathbf{j}}_m$ allocated on a dual cell facet $\tilde{A}_m \in \tilde{G}$. This process involves an averaging of the four cell permittivities $\kappa_1, \dots, \kappa_4$ to a value $\bar{\kappa}_m$ for the facet area \tilde{A}_m . The coupling constitutive relation then reads as $j_m = \bar{\kappa}_m e_m$, involving a mean current density $j_m = \hat{\mathbf{j}}_m / \int_{\tilde{A}_m} dA$ and an averaged electric field intensity $e_m = \hat{\mathbf{e}}_m / \int_{L_m} ds$.

information of the material and on the grid dimensions [10] (See Fig. 4). Since the four MGE in (11) and (12) are exact and contain only topological information, the discretization error is found to be located in the discrete constitutive material equations [10], [3].

For instance, with the definition of a maximal length of the grid cell edges h of the Cartesian grid doublet (G, \tilde{G}) the result for the coupling of the electric currents and the electric grid voltages an entry of the diagonal material matrix of conductivities is derived from

$$\begin{aligned} \frac{\int_{\tilde{A}_m} \vec{J} \cdot d\vec{A}}{\int_{L_m} \vec{E} \cdot d\vec{s}} &= \frac{\int_{\tilde{A}_m} \kappa dA}{\int_{L_m} ds} + \mathcal{O}(h^l) \\ &\approx \bar{\kappa} \frac{\int_{\tilde{A}_m} dA}{\int_{L_m} ds} = (\mathbf{M}_\kappa)_{m,m} = \frac{\hat{\mathbf{j}}_m}{\hat{\mathbf{e}}_m} \end{aligned} \quad (16)$$

for a corresponding pair of a grid voltage $\widehat{\mathbf{e}}_m$ along the edge $L_m \in G$ and the facet flux $\widehat{\mathbf{J}}_m$ through the facet $\tilde{A}_m \in \tilde{G}$. Here the error exponent l has a value $l = 2$ in the case of non-uniform grid spacing or if the cell conductivities κ_i have a different value, otherwise $l = 3$ holds [11]. The material matrix of permittivities is derived analogously.

Coordinate axis parallel orthogonal grids, where each cell is filled with only one material as shown in Fig. 4, will lead to the problem of staircase approximations of curved boundary surfaces. To overcome this problem sophisticated schemes are available with FIT for improved geometry approximation and material averaging inside the cells such as the *triangular filling* technique [12], the *tetrahedral filling* technique [13], [14] or the *Perfect Boundary Approximation* technique [15]. They allow to use computationally efficient, structured Cartesian grids, while at the same time reducing the geometry approximation error of the method (Fig. 5).

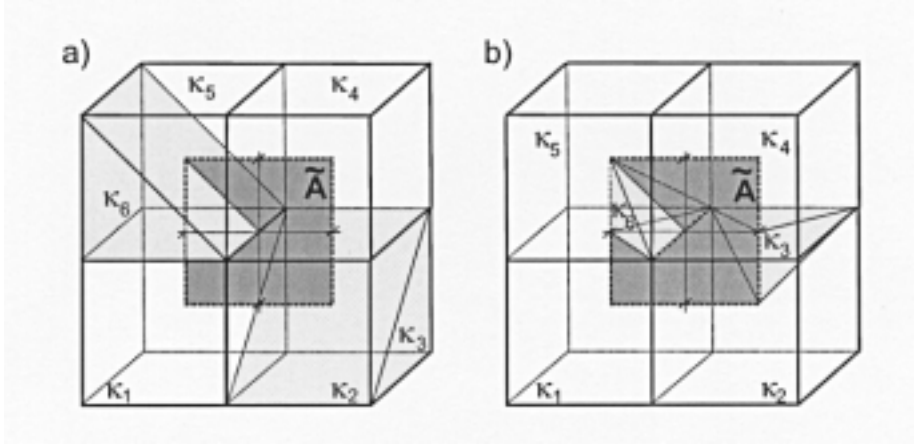


Figure 5. Both figures show an example for the averaging process of the cell material properties for the dual cell facet \tilde{A} in the presence of partial cells fillings, here for the case of different electric conductive materials within the cells. Figure a) on the left depicts the situation for triangularly partially filled cells, Figure b) on the right features tetrahedral cell subvolumes. If $|\tilde{A}_i|$ is the area of \tilde{A} cutting the cell subvolume filled with κ_i the averaged value for the conductivity on \tilde{A} is given with $\bar{\kappa} = 1/|\tilde{A}| \sum_{i=1, i \neq 3}^6 \kappa_i |\tilde{A}_i|$. Note that in both cases the cell subvolumes with κ_3 are not considered in the averaging process.

It should be noted that for non-orthogonal cell complexes the one-to-one correspondence of cell facets and dual cell edges will not necessarily coincide with a one-to-one relation of the corresponding flux

and voltage degrees of freedom. The resulting material matrices of the Nonorthogonal Finite Integration Technique (N-FIT), are symmetric, but no longer diagonal [7], [16], [17]. A treatment of dispersive, gyrotropic and non-linear material properties within the FI Technique results in numerical schemes which typically concentrate on suitable modifications of the material matrices [18], [19], [20], [21].

The basic idea for the derivation of the material matrices in FIT, as depicted in Fig. 4, is originally motivated by physical considerations. The derivation of the discrete Hodges operators for Edge-Finite-Element schemes, however, with their origin in variational formulations, involves the element-by-element quadrature of the Whitney edge shape functions w_e [22], given here e.g. for the *mass matrix* of conductivities on a tetrahedral element grid with

$$(\mathbf{M}_\kappa)_{i,j}^{\text{FE}} = \int_A \kappa w_{e_i} \cdot w_{e_j} dA. \quad (17)$$

As in the N-FIT case, the resultant material matrices of the discrete constitutive equations will be symmetric (and eventually badly conditioned for obtuse edge angles) and non-diagonal. An artificial re-diagonalization of these matrices with so-called *lumping* techniques is explained in [22] for tetrahedral meshes.

2. ALGEBRAIC PROPERTIES OF THE MATRIX OPERATORS

One of the essential properties of the discrete representation of Maxwell's equations by the boundary path and surface integral approach (hence **F**inite **I**ntegration) lies in the discrete analog to the vectoranalytical equation

$$\text{div curl} = 0, \quad (18)$$

given with the matrix equations

$$\mathbf{S}\mathbf{C} = 0, \quad (19)$$

$$\widetilde{\mathbf{S}}\widetilde{\mathbf{C}} = 0, \quad (20)$$

for the cell complex doublet $\{G, \widetilde{G}\}$. These relations result from the fact, that for all grid cells the calculation of the discrete divergence \mathbf{S} consists in the summation of the flux components. For these flux components any grid voltage (left-multiplied with the discrete *curl*-matrix \mathbf{C}) is each considered twice with different sign in the *curl*-summation giving the zero divergence result of the overall summation

(See Fig. 6). This argument from algebraic topology, where it is also used to derive the vectoranalytical identity (18) [23] directly transfers with FIT in the discrete electromagnetism, where it holds for the primal grid G and for the dual grid complex \tilde{G} and has been early recognized to be essential for conservation and stability properties.

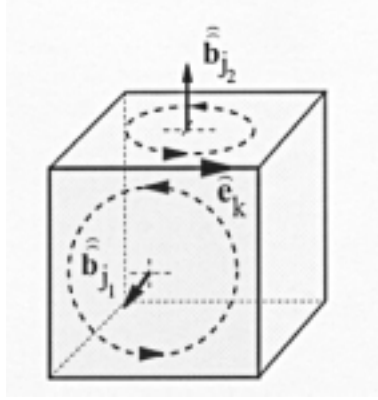


Figure 6. This sketch of the cell $V_i \in G$ demonstrates the *complex* property $\mathbf{S}\mathbf{C} = 0$ of the grid incidence matrices \mathbf{C} and \mathbf{S} . The electric grid voltage $\hat{\mathbf{e}}_k$ allocated on the boundary edge L_k occurs once with a positive and once with a negative sign in the curl-summation of the magnetic fluxes $\hat{\mathbf{b}}_{j_1}$ and $\hat{\mathbf{b}}_{j_2}$.

An important property of the Finite Integration Technique follows from the duality of the grid cell complexes G and \tilde{G} given with the relation of the discrete *curl*-matrices [24]

$$\mathbf{C} = \tilde{\mathbf{C}}^T. \quad (21)$$

Transposition of the equations (19) and (20) in combination with the identity (21) results in the discrete equations

$$\tilde{\mathbf{C}}\mathbf{S}^T = 0, \quad (22)$$

$$\mathbf{C}\tilde{\mathbf{S}}^T = 0, \quad (23)$$

both corresponding to the vector-analytical identity

$$\text{curl grad} \equiv 0. \quad (24)$$

With (22) and (23) we see that discrete fields represented as gradients of nodal potential vectors as in (14) will be exactly irrotational also on a discrete level.

The matrix equations (19), (20), (22) and (23) include only the incidence relations of the grid topology and do not contain any metrical notions [25]. They represent the typical so-called *complex property* of the simplicial grid cell complex [23]. The background mathematical connection between the discrete matrix identities (19)–(23) to the vectoranalytical identities (18) and (24) becomes readily available, when the degrees of freedom in the Finite Integration Technique are considered as *discrete differential forms* in which case the discrete grid topology matrix operators have the same effect as Cartan’s differential operator, which yields the vector-analytical operators curl, grad, div (Cf. [2]).

3. ALGEBRAIC PROPERTIES OF THE DISCRETE FIELDS

With the complex properties (19)–(23) and relation (21) arising from the duality of the dual grid doublet $\{G, \tilde{G}\}$ important existence and uniqueness results can be derived for the discrete grid fields by simply applying theoretical results from linear algebra.

An important feature of the FI-Technique as spatial discretization scheme for Maxwell’s equations is the build-in continuity equation

$$\tilde{\mathbf{S}}(\tilde{\mathbf{C}}\hat{\mathbf{h}}) = \tilde{\mathbf{S}}\left(\frac{d}{dt}\hat{\mathbf{d}} + \hat{\mathbf{j}}\right) = 0, \quad (25)$$

which corresponds to the analytic continuity equation

$$\operatorname{div}\left(\frac{\partial}{\partial t}\vec{D} + \vec{J}\right) = 0 \iff \frac{d}{dt}\mathbf{q} + \tilde{\mathbf{S}}\hat{\mathbf{j}} = 0. \quad (26)$$

The discrete continuity equation ensures that no spurious charges will occur. Such non-physical charges would result in static fields contaminating discrete transient field solutions.

If electromagnetic field processes are calculated in time domain, energy conservation of the time and space discrete system becomes of paramount importance. If this condition is violated, a necessary prerequisite for a long-term stable time integration of electromagnetic wave-propagation phenomena without artificial numerical damping is not available. For the FI-Technique the proof of this condition was given in [24], [26] for resonator structures with perfectly conducting walls.

The transformation into frequency domain for the Maxwell-Grid-Equations in (11) with $\hat{\mathbf{e}}(t) = \operatorname{Re}(\underline{\hat{\mathbf{e}}}e^{i\omega t})$ for a situation without lossy

materials ($\mathbf{M}_\kappa = 0$) and without external current excitation ($\hat{\mathbf{j}}_e = 0$) yields

$$\mathbf{C}\underline{\hat{\mathbf{e}}} = -i\omega \underline{\hat{\mathbf{b}}}, \quad (27)$$

$$\tilde{\mathbf{C}}\mathbf{M}_\nu \underline{\hat{\mathbf{b}}} = +i\omega \mathbf{M}_\varepsilon \underline{\hat{\mathbf{e}}}. \quad (28)$$

Combining these equations a general real-valued algebraic eigenvalue problem is obtained with the homogeneous curlcurl equation

$$\tilde{\mathbf{C}}\mathbf{M}_\nu \mathbf{C}\underline{\hat{\mathbf{e}}} = \omega^2 \mathbf{M}_\varepsilon \underline{\hat{\mathbf{e}}}. \quad (29)$$

Additional normalization with $\underline{\hat{\mathbf{e}}}' := \mathbf{M}_\varepsilon^{1/2} \underline{\hat{\mathbf{e}}}$ of equation (29) results in a typical real-valued eigenvalue problem

$$(\mathbf{M}_\nu^{1/2} \mathbf{C} \mathbf{M}_\varepsilon^{-1/2})^T (\mathbf{M}_\nu^{1/2} \mathbf{C} \mathbf{M}_\varepsilon^{-1/2}) \underline{\hat{\mathbf{e}}}' = \omega^2 \underline{\hat{\mathbf{e}}}'. \quad (30)$$

With the additional assumption of symmetric and positive definite material matrices \mathbf{M}_ν and \mathbf{M}_ε , the symmetry of this algebraic eigenvalue problem directly yields that all eigenvalues ω^2 of the curlcurl system matrix have to be real-valued and nonnegative. Thus a discrete field solution in time domain, which can always be decomposed into a linear combination of such undamped loss-free eigensolutions, will neither grow nor decay in time.

Another important property of the curlcurl equation without losses becomes apparent by left-multiplication of the discrete divergence matrix $\tilde{\mathbf{S}}$

$$\tilde{\mathbf{S}}\tilde{\mathbf{C}}\mathbf{M}_\nu \mathbf{C}\underline{\hat{\mathbf{e}}} = \omega^2 \tilde{\mathbf{S}}\mathbf{M}_\varepsilon \underline{\hat{\mathbf{e}}}. \quad (31)$$

Due to relation (20) of the grid incidence matrices the equation

$$\omega^2 \tilde{\mathbf{S}}\mathbf{M}_\varepsilon \underline{\hat{\mathbf{e}}} = 0, \quad (32)$$

is obtained. In case of singly connected metallic boundaries of the computational domain (32) allows the two possible solutions for the dielectric facet fluxes $\hat{\mathbf{d}} = \mathbf{M}_\varepsilon \underline{\hat{\mathbf{e}}}$ [27], [24]:

$$\hat{\mathbf{d}} : \begin{cases} \omega^2 \neq 0 & : \tilde{\mathbf{S}}\hat{\mathbf{d}} = 0 \\ \omega^2 = 0 & : \tilde{\mathbf{S}}\hat{\mathbf{d}} \neq 0 \end{cases}. \quad (33)$$

For situations in which the boundaries of perfectly electrically conductive regions of the computational domain are not singly connected, there are also non-trivial solutions $\hat{\mathbf{d}}$ for which both $\tilde{\mathbf{S}}\hat{\mathbf{d}} = 0$ and

$\omega^2 = 0$ will hold.

The original problem (29) is real-valued and symmetric and thus for simple topologies of the computational domain the eigenvectors $\widehat{\mathbf{e}}_i$ can be normalized such that they build an orthogonal set where

$$\widehat{\mathbf{e}}_i^H \widehat{\mathbf{e}}_j = \delta_{ij} \quad (34)$$

will hold. This allows the definition of two orthogonal vector subspaces of the \mathcal{R}^{3N_p} which span the vectorspace of solutions of the curlcurl equation

$$\mathcal{L}_{\text{Curl-Curl}} = \mathcal{L}_\omega \oplus \mathcal{L}_0. \quad (35)$$

This result for the eigenvalue problem yields that all rotational *dynamic* modes ($\omega \neq 0$) in \mathcal{L}_ω are orthogonal to the irrotational *static* discrete solutions for $\omega^2 = 0$.

In order to numerically control the static eigenmodes of the curlcurl matrix, it can be enhanced to a discrete ∇^2 -equation. In this case a generalized Helmholtz-equation is considered following the analytical identity

$$\nabla \times \nabla \times - \nabla \nabla \cdot = -\nabla^2. \quad (36)$$

A direct consideration of the ∇^2 -matrix on the grid cell complex pair $\{G, \tilde{G}\}$ in analogy to the analytical case is not possible, since in practice usually non-uniform material distributions have to be taken into account. The generalized Helmholtz-grid-equation reads as

$$\left[\tilde{\mathbf{C}} \mathbf{M}_\nu \mathbf{C} + \mathbf{D}_1 \tilde{\mathbf{S}}^T \mathbf{D}_2 \tilde{\mathbf{S}} \mathbf{D}_1 \right] \underline{\widehat{\mathbf{e}}} = \omega^2 \mathbf{M}_\epsilon \underline{\widehat{\mathbf{e}}}. \quad (37)$$

Depending on the proper choice of the diagonal matrices \mathbf{D}_1 and \mathbf{D}_2 in the added grad-div operator $\mathbf{D}_1 \tilde{\mathbf{S}} \mathbf{D}_2 \tilde{\mathbf{S}}^T \mathbf{D}_1$ it is possible to achieve a discretization of the ∇^2 -equation for homogeneous materials [24]. Such a possible choice consists in the definition $\mathbf{D}_1 := \mathbf{M}_\epsilon$ and $\mathbf{D}_2 := k \cdot \mathbf{D}_{\tilde{V}}^{-1}$, where $\mathbf{D}_{\tilde{V}}$ is the diagonal matrix of dual cell volumes of \tilde{G} and k is a scaling factor [24]. An alternative interpretation of the matrix \mathbf{D}_2 as diagonal norm matrix is discussed in [28] with the choice of

$$\begin{aligned} \mathbf{D}_1 &:= \mathbf{M}_\epsilon + \frac{1}{i\omega} \mathbf{M}_\kappa, \\ \mathbf{D}_2 &:= \mathbf{D}_\delta \mathbf{D}_{\tilde{V}}^{-1} \mathbf{D}_{\langle \mu \rangle}^{-1} \mathbf{D}_{\langle \varepsilon + \frac{1}{i\omega} \kappa \rangle}^{-1} \mathbf{D}_{\langle \varepsilon + \frac{1}{i\omega} \kappa \rangle}^{-H}, \end{aligned} \quad (38)$$

where the diagonal matrix (\mathbf{D}_δ) with coefficients in $\{0, 1\}$ specifies the cell vertices in regions of G , on which the grad-div operator is to be considered and especially blending out nodes in perfectly electrically conducting material. The diagonal matrix $\mathbf{D}_{\tilde{V}}$ contains the information on the cell volumes of the dual grid \tilde{G} and the diagonal matrices $\mathbf{D}_{<\varepsilon + \frac{1}{i\omega}\kappa>}$ and $\mathbf{D}_{<\mu>}$ contain the material information of the complex permittivities and permeabilities averaged over these dual cell volumes.

The background to the choice of (38) for the norm matrix lies in possibly bad condition numbers of the complete ∇^2 -matrix resulting from the different ways in which non-isotropic and inhomogeneously distributed dielectric und permeable materials are considered in both the curlcurl matrix and the grad-div matrix. In the special case of magneto-quasistatic situations, $\varepsilon + \frac{1}{i\omega}\kappa$ numerically reduces to $\frac{1}{i\omega}\kappa$ within the diagonal matrices of (38) and the addition of the effective grad-div matrix $\mathbf{M}_\kappa \tilde{\mathbf{S}}^T \mathbf{D}_2 \tilde{\mathbf{S}} \mathbf{M}_\kappa$ to an eddy current formulation allows to explicitly enforce the magneto-quasistatic continuity equation $\tilde{\mathbf{S}} \hat{\mathbf{J}} = 0$ within the whole conductive domain (Cf. [29]).

The eigenvalue problem of the discrete grad-div matrix

$$\mathbf{D}_1 \tilde{\mathbf{S}}^T \mathbf{D}_2 \tilde{\mathbf{S}} \mathbf{D}_1 \underline{\mathbf{e}} = \gamma^2 \mathbf{M}_\varepsilon \underline{\mathbf{e}}, \quad (39)$$

can be analyzed in the sense of equation (29) and then the eigenmodes for the trivial eigenvalue $\gamma^2 = 0$ correspond to the rotational eigenvectors and those of the eigenvalues $\gamma^2 \neq 0$ correspond to the irrotational eigenvectors for simple problem topologies.

The eigenvectors of the non-trivial eigenvalues $\gamma^2 \neq 0$ of (39) span a subspace $\mathcal{L}_\gamma \in \mathcal{R}^{3N_p}$, which coincides with the vectorspace Ω_0 in case of problem topologies with singly connected, perfectly electrically conducting boundaries. Thus the range of the ∇^2 -matrix can be written as a direct sum

$$\mathcal{L}_{\nabla^2} = \mathcal{L}_\omega \oplus \mathcal{L}_\gamma. \quad (40)$$

It should be noted that the eigensolutions of (39) in Ω_γ are no solutions of discrete electromagnetism, but nonetheless they may be considered as physical solutions of the discrete, stationary Schroedinger equation. In a free space region of the computational domain and with the appropriate choice of the matrices \mathbf{D}_1 and \mathbf{D}_2 the generalized ∇^2 -matrix in (37) becomes identical to the one achieved with a Finite Difference discretization of the Laplacian [24], as shown in Fig. 7.

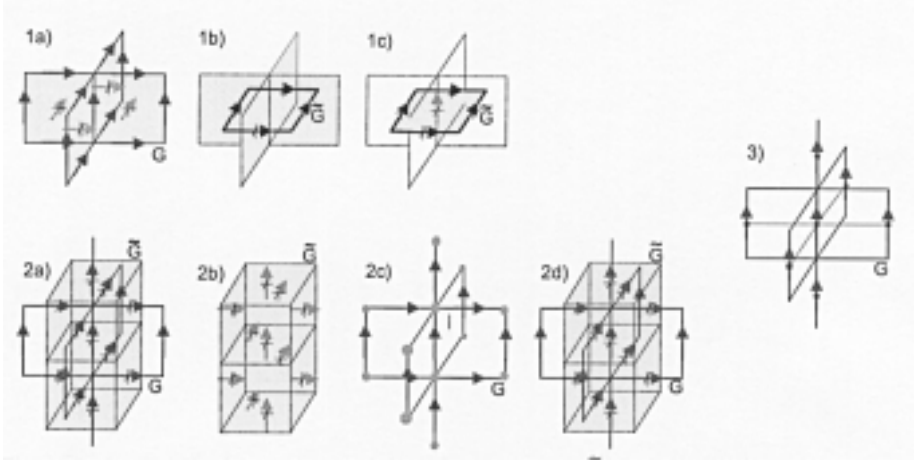


Figure 7. In the sketches 1a) to 1c) the curlcurl operator $\tilde{\mathbf{C}}\mathbf{M}_\nu\mathbf{C}$ is described: 1a) corresponds to $\tilde{\mathbf{b}} = \mathbf{C}\hat{\mathbf{a}}$, in 1b) the facet fluxes $\tilde{\mathbf{b}}$ are coupled to the magneto-motive forces on \tilde{G} by $\tilde{\mathbf{h}} = \mathbf{M}_\nu\tilde{\mathbf{b}}$ and 1c) shows, how the dual discrete curl applied to these line integrals yields the flux trough the dual facet: $\tilde{\mathbf{d}} = \tilde{\mathbf{C}}\tilde{\mathbf{h}}$. The sketches 2a)–2d) explain the discrete grad-div operator $\mathbf{D}_1\tilde{\mathbf{S}}^T\mathbf{D}_2\tilde{\mathbf{S}}\mathbf{D}_1$: 2a) applies a discrete Hodge operator $\tilde{\mathbf{d}} = \mathbf{D}_1\hat{\mathbf{e}}$ and yields the fluxes trough the facets of \tilde{G} shown in 2b). The following application of a discrete divergence yields the space a charge in each dual cell of \tilde{G} : $\mathbf{q} = \tilde{\mathbf{S}}\tilde{\mathbf{d}}$. With $\Phi = \mathbf{D}_\nu^{-1}\mathbf{q}$ the inverse of these cell volumes yields nodal potentials Φ on the nodes of G . The discrete gradient of the potential values yields grid voltages on G as depicted in 2c): $\hat{\mathbf{e}} = \tilde{\mathbf{S}}^T\Phi$. In 2d) these edge degrees of freedom on G are coupled with dual facet fluxes $\tilde{\mathbf{d}}$ applying $\tilde{\mathbf{d}} = \mathbf{D}_1\hat{\mathbf{e}}$ as in 2a). Figure 3) on the right shows the matrix stencil of the generalized ∇^2 -matrix $\tilde{\mathbf{C}}\mathbf{M}_\nu\mathbf{C} + \mathbf{D}_1\tilde{\mathbf{S}}^T\mathbf{D}_2\tilde{\mathbf{S}}\mathbf{D}_1$ for a vertical component of $\hat{\mathbf{e}}$, where \mathbf{D}_1 and \mathbf{D}_2 are chosen such that the active matrix entries resemble those of a 7-point Finite Difference matrix stencil for the ∇^2 -operator.

4. DISCRETE FIELDS IN TIME DOMAIN

So far the Maxwell-Grid-Equations only have been considered in the time continuous and space-discrete case, in which they represent large systems of ordinary differential equations and for which the Finite Integration Technique can be considered as a vertical method of lines [30]. For numerical calculations in time domain it is also necessary to

discretize the time axis of the electromagnetic process:

$$f(t), \quad t \in [t_0, t_n] \longrightarrow f(t_i), \quad t_i \in [t_0, t_n], i = 0, \dots, n \quad (41)$$

Note that the stability and charge conservation laws which were so far proven to hold for the time continuous case now also depend on the properties of the chosen numerical time marching schemes. However, the FI-theory allows also to prove these properties for a number of existing numerical schemes. Alternative formulations of other discretization approaches will not necessarily feature these time and stability properties and thus may become inaccurate or unstable within long term time integrations.

Time discrete energy conservation can be shown for the explicit FDTD leapfrog scheme [31] and for certain implicit second order Newmark-type time marching schemes [32, 33] applied to a given initial value problem with the homogeneous, non-lossy electric wave-equation

$$\mathbf{M}_\varepsilon \frac{d^2}{dt^2} \widehat{\mathbf{e}}(t) + \widetilde{\mathbf{C}} \mathbf{M}_\nu \mathbf{C} \widehat{\mathbf{e}}(t) = 0, \quad \widehat{\mathbf{e}}_0 := \widehat{\mathbf{e}}(t_0), \quad \widehat{\mathbf{e}}'_0 := \widehat{\mathbf{e}}'(t_0). \quad (42)$$

Conservation of a discrete energy [31] can be shown to hold in a time discrete sense with the relation

$$\widehat{\mathbf{e}}^{n+1,T} \mathbf{M}_\varepsilon \widehat{\mathbf{e}}^{n+1} + \widehat{\mathbf{h}}^{n+1,T} \mathbf{D}_\mu \widehat{\mathbf{h}}^{n+1} = \widehat{\mathbf{e}}^{n,T} \mathbf{M}_\varepsilon \widehat{\mathbf{e}}^n + \widehat{\mathbf{h}}^{n,T} \mathbf{D}_\mu \widehat{\mathbf{h}}^n \quad (43)$$

with the implicit two-step Crank-Nicolson scheme [34] and the one-step *Averaged-Acceleration*-scheme [11]. Within these FDiTD (*Finite Difference implicit Time Domain*) schemes [35] the time discrete solutions for both the magnetic and the electric grid voltages $\widehat{\mathbf{h}}$ and $\widehat{\mathbf{e}}$ are evaluated at the same time, whereas the explicit Leapfrog method also considers a dual-staggered grid for the time-axis.

For magneto-quasistatic problems the condition $\|d/dt \widehat{\mathbf{a}}\|_\infty \ll \|\widehat{\mathbf{j}}\|_\infty$ results in the omission of the displacement currents $d/dt \widehat{\mathbf{a}}$. A corresponding transient magneto-quasistatic formulation described in [35] and [36]

$$\mathbf{M}_\kappa \frac{d}{dt} \widehat{\mathbf{a}} + \widetilde{\mathbf{C}} \mathbf{M}_\nu \mathbf{C} \widehat{\mathbf{a}} = \widehat{\mathbf{j}}_e \quad (44)$$

is based on the modified magnetic vector potential $\widehat{\mathbf{a}} = - \int \widehat{\mathbf{e}} dt$ with $\widehat{\mathbf{b}} = \mathbf{C} \widehat{\mathbf{a}}$. The charge conservation of the magnetic field is analogously provided by the choice of the vector potential $\widehat{\mathbf{a}}$ itself and the matrix relation (19) with

$$\mathbf{S} \widehat{\mathbf{b}} = \mathbf{S} \mathbf{C} \widehat{\mathbf{a}} = 0. \quad (45)$$

The discrete magneto-quasistatic continuity equation (25) reduces to $\tilde{\mathbf{S}}\hat{\mathbf{J}} = 0$, corresponding to Kirchhoff's law of a zero current balance at nodes of electrical circuits, if one artificially restricts the currents allocated on the dual cell facets to the corresponding one-dimensional edges of the primary grid.

Thus external excitation currents $\hat{\mathbf{J}}_e$ must be of vanishing divergence, which is the case for excitation coils with closed loops or stationary current fields modelled in G . This also prohibits the use of antennas as excitation sources within these formulations, since discrete charges would have to be considered at their ends. In addition, in the conducting regions this magneto-quasistatic continuity equation $\tilde{\mathbf{S}}\hat{\mathbf{J}} = -\tilde{\mathbf{S}}\mathbf{M}_\kappa \frac{d}{dt} \hat{\mathbf{a}} = 0$ corresponds to a gauging of the vector potential, which takes into account possible jumps in the components of the vector potential normal to interfaces of materials with different conductivity. A time discretization of the non-gauged transient magneto-quasistatic formulation (44) with a θ -one-step method [33] yields a consistently singular system of equations

$$\left[\frac{1}{\theta \Delta t} \mathbf{M}_\kappa + \tilde{\mathbf{C}} \mathbf{M}_\nu \mathbf{C} \right] \hat{\mathbf{a}}^{n+1} = \left[\frac{1}{\theta \Delta t} \mathbf{M}_\kappa + \frac{1-\theta}{\theta} \tilde{\mathbf{C}} \mathbf{M}_\nu \mathbf{C} \right] \hat{\mathbf{a}}^n + \hat{\mathbf{J}}_e^{n+1} + \frac{1-\theta}{\theta} \hat{\mathbf{J}}_e^n, \quad (46)$$

which have to be solved repeatedly. Nonlinear ferromagnetic material behaviour modelled in $\mathbf{M}_\nu(\hat{\mathbf{a}}^{n+1})$ can be tackled with linearization techniques and the resulting linear systems will have a similar structure to (46) [37]. Left multiplication of (46) with $\tilde{\mathbf{S}}$ shows that the continuity equation for the eddy currents will be enforced in a time discretized sense with

$$\tilde{\mathbf{S}} \mathbf{M}_\kappa \hat{\mathbf{a}}^{n+1} = \tilde{\mathbf{S}} \mathbf{M}_\kappa \hat{\mathbf{a}}^n = \dots = \tilde{\mathbf{S}} \mathbf{M}_\kappa \hat{\mathbf{a}}^0. \quad (47)$$

Note, that for the magneto-quasistatic formulation with its continuity equation $\tilde{\mathbf{S}}\hat{\mathbf{J}} = 0$ also the condition $d/dt \mathbf{q} = 0$ is implied from the discrete continuity condition of the complete set of Maxwell-Grid-Equations. The result $d/dt \mathbf{q} = 0$ provides, that no spurious irrotational solution parts will accumulate in $\hat{\mathbf{a}}$ in the non-conductive regions arising from the spatial discretization itself. If in addition a solution method for the consistently singular system (46) with a *weak gauging property*, as featured by e.g. the conjugate gradient method [35], is applied with a zero start vector of the iteration, the relation $\tilde{\mathbf{S}} \mathbf{D} \hat{\mathbf{a}}^{n+1} = 0$ will hold for exact arithmetics. Thus the charge conservation property of the FI Technique also becomes an integral part of the non-gauged formulation (44) itself.

5. CONCLUSION

The Finite Integration Technique is a discretization method which transforms Maxwell's equations onto a dual grid cell complex, resulting in a set of discrete matrix equations. The degrees of freedom collected in the vectors of this discretization scheme, typically consist in physically measurable, *integral* quantities such as voltages, currents or charges. This discretization approach results in sparse integer matrices \mathbf{C} , $\tilde{\mathbf{C}}$, \mathbf{S} , $\tilde{\mathbf{S}}$ which only contain information on the incidence relations of the dual cell complex. This mere restriction to topological information of the simplicial grid is responsible for the typical complex property $\mathbf{SC} = 0$ and $\tilde{\mathbf{S}}\tilde{\mathbf{C}} = 0$. In connection with the relation $\mathbf{C} = \tilde{\mathbf{C}}^T$ due to the duality of the grid pair and with symmetric and positive definite material matrices the topologically related relations of these incidence matrices allow to prove energy and charge conservation of the spatially discretized formulations. For the homogenous undamped curlcurl equation a real-valued spectrum with orthogonal subspaces for static and dynamic eigenmodes was shown to exist. In addition, the algebraic properties of the MGE of FIT also allow to prove charge and energy conservation within time discrete schemes such as the explicit Leapfrog FDTD scheme or certain second order implicit methods. Implicit time integration schemes can also be applied to non-gauged magneto-quasistatic formulations, which yield singular matrix systems that still can be numerically tackled due to their consistency given with the FIT approach. These results clearly distinguish these time integration schemes from many alternative methods which do not rely on space and time stability and thus may become unstable or inaccurate within long term calculations.

REFERENCES

1. Weiland, T., "A discretization method for the solution of Maxwell's equations for six-component fields," *Electronics and Communications AEÜ*, Vol. 31, No. 3, 116–120, 1977.
2. Tonti, E., "On the geometrical structure of electromagnetism," *Gravitation, Electromagnetism and Geometrical Structures*, G. Ferraese (ed.), 281–308, Pitagora, Bologna, 1996.
3. Bossavit, A., L. Kettunen, and T. Tarhassaari, "Some realizations of a discrete Hodge operator: A reinterpretation of the finite element technique," *IEEE Transactions on Magnetics*, Vol. 35, 1494–1497, May 1999.
4. Teixeira, F. L. and W. C. Chew, "Lattice electromagnetic theory

- from a topological viewpoint,” *Journal of Mathematical Physics*, Vol. 40, No. 1, 169–187, 1999.
5. Nédélec, J. C., “Mixed finite elements in R^3 ,” *Numerische Mathematik*, No. 35, 315–341, 1980.
 6. van Rienen, U. and T. Weiland, “Triangular discretization method for the evaluation of RF-fields in cylindrically symmetric cavities,” *IEEE Transactions on Magnetics*, Vol. MAG-21, No. 6, 2317–2320, 1985.
 7. Schuhmann, R. and T. Weiland, “A stable interpolation technique for FDTD on nonorthogonal grids,” *International Journal on Numerical Modelling*, Vol. 11, 299–306, May 1998.
 8. Thoma, P. and T. Weiland, “A consistent subgridding scheme for the finite difference time domain method,” *International Journal of Numerical Modelling*, Vol. 9, 359–374, 1996.
 9. Chen, W. K., *Graph Theory and It’s Engineering Applications*, Vol. 5, Advanced Series in Electrical and Computer Engineering, World Scientific, Singapor, 1996.
 10. Weiland, T., “Time domain electromagnetic field computation with finite difference methods,” *International Journal of Numerical Modelling: Electronic Networks, Devices and Fields*, Vol. 9, 259–319, 1996.
 11. Clemens, M., “Zur numerischen Berechnung zeitlich langsam-veränderlicher elektromagnetischer Felder mit der Finiten-Integrations-Methode,” Ph.D. thesis, Technische Universität Darmstadt, 1998.
 12. Weiland, T., “Lossy waveguides with arbitrary boundary contour and distribution of material,” *Electronics and Communications AEÜ*, Vol. 33, 170, 1979.
 13. Müller, W. and W. Wolff, “Ein Beitrag zur numerischen Berechnung von Magnetfeldern,” *Elektrotechnische Zeitung*, Vol. 96, 269–273, 1975.
 14. Müller, W., J. Krüger, A. Jacobus, R. Winz, T. Weiland, H. Euler, U. Kamm, and W. R. Novender, “Numerical solution of 2- and 3-dimensional nonlinear field problems by means of the computer program PROF1,” *Archiv für Elektrotechnik*, Vol. 65, 299–307, 1982.
 15. Krietenstein, B., P. Thoma, R. Schuhmann, and T. Weiland, “The perfect boundary approximation technique facing the big challenge of high precision computation,” *Proceedings of the 19th LINAC Conference*, Chicago, August 1998.
 16. Schuhmann, R. and T. Weiland, “FDTD on nonorthogonal

- grids with triangular fillings," *IEEE Transactions on Magnetics*, Vol. 35, 1470–1473, May 1999.
17. Clemens, M., M. Hilgner, R. Schuhmann, and T. Weiland, "Transient eddy current simulation using the nonorthogonal finite integration technique," *Conference Records of the CEFC 2000, Milwaukee*, 385, 2000. Full paper submitted to *IEEE Transactions on Magnetics*.
 18. Gutschling, S., "Zeitbereichsverfahren zur simulation elektromagnetischer felder in dispersiven materialien," Ph.D. thesis, Technische Universität Darmstadt, 1998.
 19. Gutschling, S., H. Krüger, H. Spachmann, and T. Weiland, "FIT-formulation for nonlinear dispersive media," *International Journal on Numerical Modelling*, Vol. 12, 81–92, 1999.
 20. Krüger, H., H. Spachmann, and T. Weiland, "FIT-formulation for gyrotropic media," *Proceedings of the ICCEA1999*, Torino, Italy, 1999.
 21. Clemens, M., S. Drobny, and T. Weiland, "Time integration of slowly-varying electromagnetic field problems using the finite integration technique," *Proceedings of the ENUMATH 97*, 246–253, Heidelberg, 1999.
 22. Bossavit, A. and L. Kettunen, "Yee-like schemes on a tetrahedral mesh, with diagonal lumping," *International Journal of Numerical Modelling: Electronic Networks, Devices and Fields*, Vol. 12, No. 1/2, 129–142, 1999.
 23. Jänich, K., *Vektoranalysis*, 191–222, Springer Lehrbuch, Springer, 1993.
 24. Weiland, T., "On the unique numerical solution of Maxwellian eigenvalue problems in three dimensions," *Particle Accelerators*, Vol. 17, 227–242, 1985.
 25. Tonti, E., "Discrete formulation of the electromagnetic field," University Trieste, 34127 Trieste, Italy, 1998.
 26. Thoma, P. and T. Weiland, "Numerical stability of finite difference time domain methods," *IEEE Transactions on Magnetics*, Vol. 34, No. 5, 2740–2743, 1998.
 27. Schmitt, D., "Zur numerischen berechnung von resonatoren und wellenleitern," Ph.D. thesis, Technische Hochschule Darmstadt, 1994.
 28. Hahne, P., "Zur numerischen berechnung zeitharmonischer elektromagnetischer felder," Ph.D. thesis, Technische Hochschule Darmstadt, 1992.
 29. Bossavit, A., "'stiff' problems in eddy-current theory and the

- regularization of Maxell's equations," in *Conference Records of the CEFC 2000, Milwaukee*, 497, 1997. Full paper submitted to *IEEE Transactions on Magnetism*.
30. Großmann, C. and H.-G. Roos, *Numerik partieller Differentialgleichungen*, B. G. Teubner Verlag, Stuttgart, 1994.
 31. Schuhmann, R. and T. Weiland, "Conservation of discrete energy and related laws in the finite integration technique," this volume.
 32. Zienkiewicz, O. C., "A new look at the Newmark, Houbolt and other time stepping formulas. A weighted residual approach," *Earthquake Engineering and Structural Dynamics*, No. 5, 413–418, 1977.
 33. Zienkiewicz, O. C., W. L. Wood, N. H. Hine, and R. L. Taylor, "A unified set of single step algorithms; part 1," *Int. J. for Num. Meth. in Eng.*, Vol. 20, 1529–1552, 1984.
 34. Monk, P., "A mixed method for approximating Maxwell's equations," *SIAM J. Numer. Anal.*, Vol. 28, 1610–1634, December 1991.
 35. Clemens, M. and T. Weiland, "Transient eddy current calculation with the FI-method," *IEEE Transactions on Magnetism*, Vol. 35, 1163–1166, May 1999.
 36. Clemens, M. and T. Weiland, "Numerical algorithms for the FDiTD and FDFD simulation of slowly-varying electromagnetic fields," *Int. J. Numerical Modelling, Special Issue on Finite Difference Time Domain and Frequency Domain Methods*, Vol. 12, No. 1/2, 3–22, 1999.
 37. Drobny, S., M. Clemens, and T. Weiland, "Dual nonlinear magnetostatic formulations using the finite integration technique," *Conference Records of the CEFC 2000, Milwaukee*, 392, 2000. Full paper submitted to *IEEE Transactions on Magnetism*.